Edge contraction in persistence-generated discrete Morse vector fields

Tamal K. Dey*[1] and Ryan Slechta†[1]

[1]Department of Computer Science and Engineering, The Ohio State University, Columbus, OH 43210, USA.

May 19, 2018

Abstract

Recently, discrete Morse vector fields have been shown to be useful in various applications. Analogous to the simplification of large meshes using edge contractions, one may want to simplify the cell complex K on which a discrete Morse vector field $V(K)$ is defined. To this end, we define a gradient aware edge contraction operator for triangulated 2-manifolds with the following guarantee. If $V(K)$ was generated by a specific persistence-based method, then the vector field that results from our contraction operator is exactly the same as the vector field produced by applying the same persistence-based method to the contracted complex. An implication of this result is that local operations on $V(K)$ are sufficient to produce the persistence-based vector field on the contracted complex. Furthermore, our experiments show that the structure of the vector field is largely preserved by our operator. For example, 1-unstable manifolds remain largely unaffected by the contraction. This suggests that for some applications of discrete Morse theory, it is sufficient to use a contracted complex.

1 Introduction

Morse theory has become a subject of interest due to its ability to completely describe the flow of a class of vector fields defined over a manifold [22]. Such a description is useful for scientific purposes, as it improves understanding of the behavior of the underlying *Morse function* - a smooth function without any degenerate critical points. This description is called the *Morse-Smale complex*, and it is uniquely defined for a manifold-Morse function pair. A Morse-Smale complex is a decomposition of the manifold into regions of similar flow, called *cells*. Each point on the given manifold is either critical or lies on an *integral line* between a unique pair of critical points. An integral line is a path between (but not including) a pair

*dey.8@osu.edu
†slechta.3@osu.edu

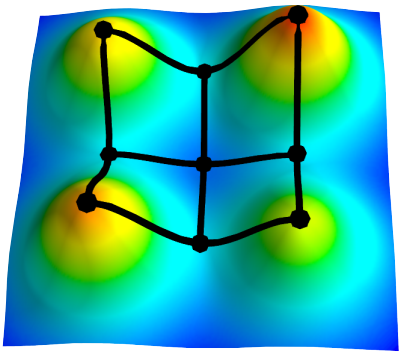

Figure 1: An example of a smooth Morse-Smale complex with four Morse cells bounded by black curves connecting a maximum (peaks) to two saddles and each saddle to a minimum (pit).

of critical points with tangent vectors that agree with the gradient of the Morse function at all points. Hence, a cell in the Morse-Smale decomposition is precisely the set of all points in a manifold which lie on an integral line between two given critical points. We include an example of a Morse-Smale complex in Figure 1. Such a topological characterization of vector fields is important in areas including fluid dynamics and aerodynamics, when it is necessary to work with continuous functions [21].

However, experimental data is not usually collected in the form of Morse functions. This makes applying smooth techniques problematic. The first attempt at constructing a discrete version of the Morse-Smale complex was done by *Edelsbrunner et. al.* for piecewise linear 2-manifolds, but their techniques are fairly involved [10]. Forman's discrete Morse theory, the focus of this paper, establishes an analog of the Morse-Smale complex for functions defined over cell complexes [14, 13]. For simplicity, this paper only considers simplicial complexes. Key to discrete Morse theory is a class of functions called *discrete Morse functions*. Analogous to the smooth case, these functions induce a gradient vector field on their domain. Forman's theory is strictly combinatorial, and most of its results pertain to manipulating discrete vectors. No derivatives are required. Despite this, discrete Morse theory still contains a number of concepts analogous to structures in classical Morse theory. Among these are notions of *critical simplices* and *gradient paths*, which can be thought of as corresponding to critical points and integral lines, respectively. In the discrete case, the highest dimensional cells may serve as local maxima when they are critical, and critical vertices serve as local minima. When critical, all other simplices are the equivalent of saddles. Hence, gradient paths connect higher dimensional simplices to lower dimensional simplices. These gradient paths allow the computation of a Morse-Smale complex for triangulated manifolds, with structure resembling that of the smooth Morse-Smale complex. Forman's theory has found applications in a variety of areas, including cosmology, terrain analysis, and road network reconstruction [3, 24, 25, 7, 8].

Discrete Morse functions are defined over all simplices in a simplicial complex, whereas scientific data can usually be thought of as a height function on a set of points. The canonical example of this is terrain modeling: on some collection of points, one has elevation data, but no information on the behavior of the terrain between the sampled points. A simplicial

complex can be generated over the terrain by taking some triangulation of the sampled points. These points are the vertices of the simplicial complex, and they are the only simplices in the complex that are associated with a function value. While interpolation methods could be used to assign function values to higher dimensional simplices, this will only be a discrete Morse function on the rarest of occasions. Various techniques have been proposed to compute a discrete Morse vector field from an input height function defined over a complex's vertex set [24, 15, 23, 5, 18]. We choose to use an algorithm presented by *Bauer et. al.* which, given any triangulated 2-manifold, outputs a discrete Morse gradient vector field on the triangulation [2]. This algorithm is advantageous in that it is simple (see [8] for further simplification) to implement and very intuitive. It takes as input two parameters: a filtration, or a total ordering on the simplices of K often referred to as $\prec$, and a tuning parameter, δ, which influences the number of remaining critical simplices. When $\delta = \infty$, their algorithm is proven to output a discrete Morse vector field which minimizes the number of critical simplices.

This δ value tunes the output according to the persistence associated with each edge. The idea behind persistence is that if K_0 is chosen to be an empty complex, and K_i is the complex that results after adding the ith simplex under $\prec$ to K_{i-1}, then each added simplex either creates or destroys a homological class. Such a creation or destruction corresponds to a change in the topology of the complex. Persistent homology provides a description of this changing topology by capturing the lifetime – or the "persistence" – of the various classes. For a more thorough treatment of persistent homology, we encourage the reader to consult [11] or [9]. Each edge is then either associated with the persistence of the class which it creates or destroys. The algorithm by *Bauer et. al.* leaves those edges with persistence $\geq \delta$ as critical.

Triangulated 2-manifolds, together with the discrete Morse gradient vector fields defined on them, can become quite large. An obvious approach to controlling size is to arbitrarily contract edges in the original manifold prior to computing the discrete Morse vector field. Such a procedure is problematic, because a contraction operator that is oblivious to vector field dynamics may lead to a drastically different vector field on the contracted manifold. An alternative is to contract edges in the triangulation and modify the original vector field slightly to fit the new complex. To make contraction as efficient as possible, it is important that the vector field only needs to be modified local to the contraction. Work in this area was initiated by *Iuricich and De Floriani*, who established such a contraction operator in the context of storing a discrete Morse vector field at several resolutions [16]. However, their criteria for a permissible contraction are fairly strong, in that they disallow circumstances where contraction could be permitted. In particular, they do not permit contractions that destroy critical simplices. This paper establishes a contraction operator which subsumes their criteria and, more importantly, comes with additional mathematical guarantees. If one were to run the algorithm by *Bauer et. al.* on the contracted manifold with the same δ that generated the original discrete Morse vector field, then the output vector field is guaranteed to be the same as the one which results from the contraction operator. The new operator is established in Section 4, while a formalization of the guarantee is in Section 5.

An *unstable* 1*-manifold* is the set of all simplices that can be reached by gradient paths originating at a critical edge. An example can be seen in Figure 2. Various authors have found uses for these manifolds [24, 25, 7, 8, 5]. These unstable manifolds largely preserve their structure under contraction. Hence, it is often sufficient to use a much coarser complex

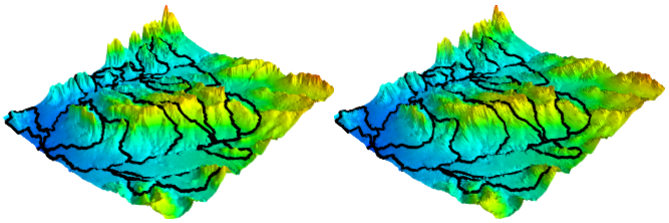

Figure 2: An example of unstable 1-manifolds on a terrain near Los Alamos, New Mexico before (left) and after (right) 400,000 edge contractions. Note that there is very little difference in the paths of the unstable manifolds.

for the previous applications. In Section 6, we demonstrate this approach on a road network reconstruction application as a proof of concept. In addition, the new contraction operator is more general than the state of the art, and experiments are presented comparing coarsest possible representations. The paper concludes in Section 7 with a discussion on future directions for research.

2 Discrete Morse theory

We now provide background in Forman's discrete Morse theory. For a more thorough treatment, we refer the reader to [14] or [13]. In this section, we define K to be a simplicial complex. Fundamental to discrete Morse theory are *discrete Morse functions*. A function $f : K \to \mathbb{R}$ is a discrete Morse function if it satisfies the following two conditions for all simplices $\sigma \in K$:

$$|\{\tau <_1 \sigma \mid f(\tau) \geq f(\sigma)\}| \leq 1 \tag{1}$$
$$|\{\tau >_1 \sigma \mid f(\tau) \leq f(\sigma)\}| \leq 1 \tag{2}$$

where we write $\tau <_1 \sigma$ or $\sigma >_1 \tau$ if τ is a facet (a face of codimension 1) of σ. Forman proved that both of these quantities cannot be positive for the same simplex.

Lemma 1. *For every simplex $\sigma \in K$, $|\{\tau <_1 \sigma \mid f(\tau) \geq f(\sigma)\}| = 0$ or $|\{\tau >_1 \sigma \mid f(\tau) \leq f(\sigma)\}| = 0$.*

These conditions also give a concept of a critical simplex.

Definition 2. *A simplex σ is critical if $|\{\tau <_1 \sigma \mid f(\tau) \geq f(\sigma)\}| = 0$ and $|\{\tau >_1 \sigma \mid f(\tau) \leq f(\sigma)\}| = 0$*

Critical simplices will play a similar role in computing the Morse-Smale complex as they do in the smooth case.

Discrete Morse theory defines the Morse-Smale complex in terms of gradient vector fields. Such a gradient vector field is constructed as one might expect: if $\tau <_1 \sigma$ and $f(\tau) \geq f(\sigma)$, where f is a discrete Morse function, then the discrete Morse gradient field contains a vector with tail at τ and head at σ. In such a case, we say that τ "targets" σ. Note that Lemma 1 implies the following.

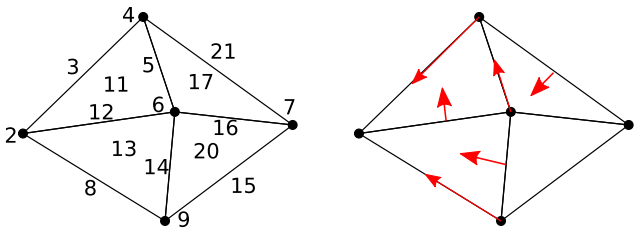

Figure 3: An example of a discrete Morse function (left) with its induced gradient vector field (right). Those simplices which are neither the head nor tail of a gradient vector are precisely those simplices which are critical.

Corollary 3. *Every simplex $\sigma \in K$ satisfies exactly one of the following:*

1. *σ is the head of exactly one vector and the tail of no vector*
2. *σ is the tail of exactly one vector and the head of no vector*
3. *σ is neither the head nor tail of any vectors.*

Equivalently, a simplex can participate in at most a single discrete Morse vector. In Figure 3, we provide an example of a vector field induced by a discrete Morse function. Note that it is not immediate that an arbitrary assignment of vectors satisfying Corollary 3 necessarily corresponds to a vector field induced by a discrete Morse function. An arbitrary assignment of these vectors is called a *discrete vector field*. A vector field induced by a discrete Morse function is a *discrete Morse vector field*. To establish which discrete vector fields are discrete Morse vector fields, it is necessary to define a notion of "flow" induced by these vector fields. Forman formalizes this notion by defining the analog of the integral line.

Definition 4 (V-Path). *A sequence of simplices $a_0, b_0, a_1, b_1, \ldots, a_n, b_n, a_{n+1}$ is a V-Path if for each $i = 0, 1, \ldots, n$, there is a discrete Morse vector from a_i to b_i, and $a_{i+1} <_1 b_i$, $a_{i+1} \neq a_i$.*

Frequently, V-paths are referred to as *gradient paths*. A gradient path is *closed* if $a_0 = a_{n+1}$. Closed gradient paths can also be called *cycles*. It is standard to abuse notation such that the last simplex of the path is not required to be of the same dimension as the first. That is, V-Paths are permitted to end on b_n instead of a_{n+1}. An example of such a gradient path can be seen on the left in Figure 4, where there are gradient paths from the only critical triangle to two critical edges. The following Theorem, due to Forman, establishes which discrete vector fields are induced by a discrete Morse function.

Theorem 5 (Cyclicity). *A discrete vector field is a discrete Morse vector field if and only if it contains no nontrivial closed V-Paths.*

Hence, preventing any closed V-Paths is paramount when developing a contraction operator. In developing his theory, Forman also developed a notion of "canceling" critical simplices. For a critical simplex σ to cancel critical simplex τ, it is required that they differ in dimension by 1. Hence, assume $\dim(\sigma) = \dim(\tau) + 1$. Simplices τ and σ can cancel each other if there exists a gradient path from σ to τ. An example can be seen in Figure 4. The cancellation operator amounts to reversing the direction of the arrows in the gradient path.

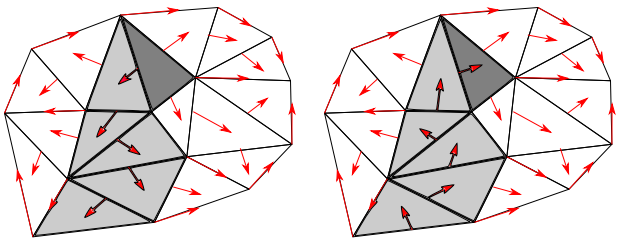

Figure 4: An example of a discrete Morse gradient field before (left) and after (right) the cancellation of a critical triangle with a critical edge along the path indicated with shades of gray. Note that on the left, the dark gray triangle is critical, whereas on the right, it is targeted by an edge.

Hence, after canceling, there is a V-path from τ to σ instead of the reverse. However, this is potentially problematic. In the image on the left of Figure 4, there are gradient paths from the dark grey critical triangle to two different critical edges. Should the other critical edge have been chosen to be canceled, then there would have been a closed gradient path in the resulting vector field. Hence, prior to cancellation, it is necessary to ensure that cancellation will not create a cycle. As we have previously discussed, for a complex of dimension n, critical n-simplices correspond to local maxima and critical vertices correspond to local minima. Canceling a critical n-simplex then has the effect of removing a local maximum. In this sense, the cancellation operation is effectively a morphology simplification operator.

3 Persistence based discrete Morse vector fields

3.1 2-manifolds

We describe an algorithm by *Bauer et. al.* [2] which uses persistence to construct a discrete Morse vector field on a triangulated 2-manifold K. The algorithm is based on the work of *Attali et. al.* [1] who describe a method to compute persistence in linear time on filtered graphs. Inputs to the algorithm are a parameter δ and a filtration $K_0 \subseteq K_1 \subseteq \ldots \subseteq K_m = K$ where each K_i is itself a subcomplex of K. Note that this filtration can be thought of as a sequence of sublevel sets of K. Hence, the filtration induces a height function

$$h : K \to \mathbb{R}$$

where, if $\sigma \in K_i$ and $\sigma \notin K_{i-1}$, $h(\sigma)$ corresponds to the height value assigned to K_i. The simplices are assigned a persistence value, which is equal to the lifetime of the homological class they create or destroy. If a simplex σ creates a homological class that is destroyed by a simplex τ coming later in the filtration, we say (σ, τ) is a *persistence pair* and the *persistence* of σ and τ is $h(\tau) - h(\sigma)$. Notice that a homology class created by σ may never be destroyed, in which case, its persistence is assigned to be ∞.

The algorithm has the advantage of being incredibly simple, and tunable to generate a varying number of critical simplices by parameter δ. Those edges with persistence $\geq \delta$ remain critical. Pseudocode is available in Algorithm 1. The reader may wish to consult [2] (and [8] for further simplification) for more details.

It is important to note that the algorithm requires a total order on the simplices of K. This is given by the filtration. In the event that $|K_i \setminus K_{i-1}| > 1$, we break ties by placing the lowest dimensional simplices first, and then arbitrarily breaking ties within each dimension. This induces a new filtration where each sublevel set adds exactly one simplex. Hence, we assume that for the initial filtration, $|K_i \setminus K_{i-1}| \leq 1$. We refer to the total order induced by such a filtration as $\prec$.

The algorithm proceeds in four steps, the first two of which are a modified version of Kruskal's algorithm. The first step is to build a minimum spanning forest on the graph induced by the triangulated manifold under the aforementioned total order. When an edge e is introduced to the minimum spanning forest, e joins two trees rooted at vertices v_0 and v_1. Whichever of v_0 or v_1 has lower height value is then chosen to be the root of the new combined tree. The edge e pairs with the vertex that has the larger height value and thus the persistence associated with edge e is exactly $h(e) - \max\{h(v_0), h(v_1)\}$. This is because introducing edge e kills one of the two 0-cycles, and the class of the younger cycle (occurring later in the filtration) is chosen to die. Should the persistence of the edge be greater than or equal to δ, the two trees remain distinct but are symbolically connected to enable computing persistence for the remaining edges. Effectively, we maintain two forests. One which constructs a minimum spanning tree, and one which maintains a forest that is equivalent to the minimum spanning tree except missing those edges with associated persistence $\geq \delta$.

The second step is a similar procedure on the graph that is induced by thinking of the triangles as vertices connected by edges. However, it is important to remove any boundary that may exist in the complex. This procedure is depicted in Figure 6. Each boundary edge is assigned a new triangle with a very high height value. The same modified version of Kruskal's algorithm is then used to build a maximum spanning forest on this graph with edges disjoint from the previous minimum spanning tree. Similar to the previous case, when an edge e is introduced in the maximum spanning tree, e joins two trees rooted at triangles t_0 and t_1. Unlike the previous case, the root of the new combined tree is whichever of t_0 or t_1 has a greater height value. The persistence associated with e is then $\min\{h(t_0), h(t_1)\} - h(e)$. Again, if the persistence associated with e is greater than or equal to δ, then the trees remain disjoint.

Following the completion of this stage, there are a series of disjoint vertex/edge and edge/triangle trees, which are disconnected from each other via edges e which have associated persistence greater than δ. Each tree is either rooted at a minimum vertex or a maximum triangle. These minima and maxima will be the only simplices in each tree which remain critical. The third and fourth steps are to assign discrete Morse vectors. This is done by leaving the root critical, and propagating up the tree, in the case of a vertex/edge tree, or down the tree, in the case of triangle/edge trees. An example can be seen in Figure 5.

3.2 Guarantees

The following theorems pertaining to the algorithm follow from work in [2] and [1].

Theorem 6. *For a triangulated 2-manifold K, Algorithm 1 outputs a valid discrete Morse vector field on K.*

Algorithm 1 Computing a gradient vector field on a 2-manifold with boundary from a filtration

1: **procedure** CONSTRUCT-VECTOR-FIELD(K, δ, f) ▷ K a simplicial complex, δ persistence limit, $f : K \to \mathbb{R}$
2: $V, E, T \leftarrow Separate(K)$ ▷ Separate K into vertices, edges, triangles
3: MODIFIED-KRUSKAL'S-MINST(E)
4: REMOVE-BOUNDARY(V,E,T)
5: MODIFIED-KRUSKAL'S-MAXST(V,E,T)
6: ASSIGN-VECTORS-VERTICES(V)
7: ASSIGN-VECTORS-TRIANGLES(T)

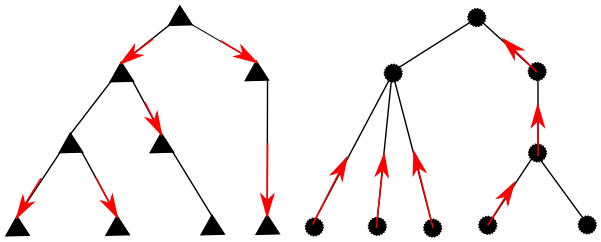

Figure 5: An example of how vectors are assigned to edges in `Assign-Vectors-Triangles`(left) and `Assign-Vectors-Vertices`(right). Those edges which remain critical are the ones with associated persistence greater than or equal to δ.

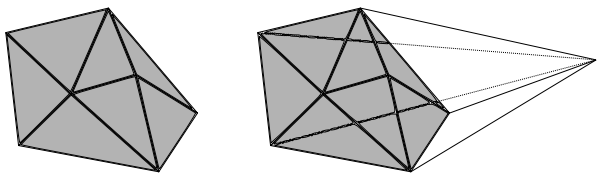

Figure 6: An example of a triangulated 2-manifold before (left) and after (right) the `Remove-Boundary` procedure.

A less immediate result concerns the optimality of the algorithm.

Theorem 7. *If K is a triangulated 2-manifold and $\delta = \infty$ then Algorithm 1 outputs an optimal discrete Morse vector field on K. That is, no additional simplices may be cancelled.*

3.3 Related Algorithms

Several authors have developed algorithms for computing a discrete Morse vector field on 2-manifolds. *Lewiner et. al.* invented an algorithm which can construct an optimal discrete Morse function over a 2-manifold in [19] and extended it to achieve near-optimal results on arbitrary complexes in [20]. Their algorithm is quite similar to the one provided in the previous subsection when $\delta = \infty$, but it does not take a filtration or a height function as input, and thus it is not suitable for scalar field analysis. *Robins et. al.* have proposed a homotopy extension-based algorithm for computing discrete Morse vector fields on cubical complexes in 2 and 3 dimensions [23]. Their algorithm is proven to be optimal for specific classes of cubical complexes. It has been adapted for simplicial complexes in [12, 26]. *King et. al.* and *Čomić et. al.* have both also presented algorithms for computing a discrete Morse gradient field from a height function [18, 4]. None of these algorithms are tunable with some δ, which enables testing our contraction scheme on vector fields with a varying amount of critical simplices.

4 Edge contraction

4.1 Preliminaries and definitions

We now establish criteria for a contraction operator which, upon contraction, outputs the same discrete Morse vector field as the vector field that would be obtained by running Algorithm 1 on the contracted complex. Throughout this section, we label an initial triangulated 2-manifold, possibly with boundary, as K. Similarly, we will often refer to the resulting manifold after contraction as K'. As each simplex in K is equipped with a height value, we define the function

$$h : K \to \mathbb{R}$$

to refer to this quantity. The edge to be contracted is denoted as $e = \{u, v\} \in K$. We label u and v such that $u \prec v$ (that is, u occurs before v in the input filtration).

In addition, we label various simplices "near" the contracting edge, e. See Figure 7 for reference. Those simplices containing $\{u, v\}$ as a face are called *vanishing simplices*. In Figure 7 these are simplices $\{a, u, v\}$, $\{b, u, v\}$, and $\{u, v\}$. We say a simplex is a *mirrored simplex* if it is not vanishing, but is the facet of vanishing simplex. In Figure 7, these are edges $\{a, u\}$, $\{a, v\}$, $\{b, u\}$, $\{b, v\}$ and vertices $\{u\}$ and $\{v\}$. Each mirrored simplex is paired with its mirror. If σ is a mirrored simplex, then the mirror of σ is the simplex obtained by considering the convex hull of σ but swapping out u for v (or vice versa). Therefore, in Figure 7, $\{a, u\}$ and $\{a, v\}$ are each others' mirrors with respect to the edge e. Similarly, $\{b, v\}$ and $\{b, u\}$ are a pair of mirrors, as are $\{u\}$ and $\{v\}$. *Adjacent simplices* are those simplices which are neither vanishing simplices nor mirrored simplices, but contain at least

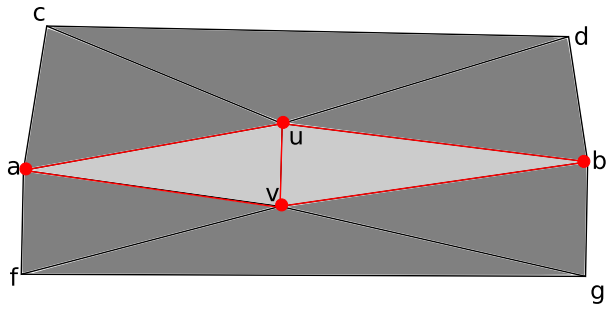

Figure 7: A reference figure when considering to contract edge $\{u, v\}$. Local triangles are highlighted in light grey while local edges and vertices are highlighted in red.

one mirrored simplex as a face. In Figure 7, these are triangles $\{a, c, u\}$, $\{b, d, u\}$, $\{a, f, v\}$, $\{b, g, v\}$, and edges $\{c, u\}$, $\{d, u\}$, $\{f, v\}$, and $\{g, v\}$. Finally, *bystander simplices* are those simplices which are a face of a mirrored simplex, but not a mirror themselves. In Figure 7, these are the vertices $\{a\}$ and $\{b\}$. We refer to a simplex that is vanishing, mirrored, or a bystander as being *local* to the edge being contracted. Equivalently, local simplices are those σ which are either vanishing or the face of a vanishing simplex. We aim to establish a contraction operator which preserves the validity of the discrete Morse vector field while only considering simplices local to the edge that is being contracted. In addition, we will define our contraction operator such that our contractions are faithful to the underlying total order.

4.2 Contraction operator

We now define the contraction operator, viewed as simplicial map

$$\xi_{\{\mathrm{u,v}\}} : K \to K'$$

where $\{u, v\}$ is the edge to be contracted. For notational ease, we assume that $u \prec v$. Naturally, only local simplices are affected by a contraction, so $\xi_{\{\mathrm{u,v}\}}$ can be viewed as the identity on all nonlocal simplices. For local simplices, more care is needed. Mirrored simplices are going to be "merged" into a single simplex, so it is necessary to choose which one will survive. Rigorously, if σ_1, σ_2 are mirrors, where u is a constituent vertex of σ_1, then $\xi_{\{\mathrm{u,v}\}}(\sigma_1) = \xi_{\{\mathrm{u,v}\}}(\sigma_2) = \sigma_1$. In effect, we choose the mirror which occurs earlier in the total order as the "survivor," while ensuring that it contains the surviving vertex. Hence, $\xi_{\{\mathrm{u,v}\}}(\sigma_1) = \xi_{\{\mathrm{u,v}\}}(\sigma_2)$ assumes the first position in the total order occupied by σ_1 or σ_2. If σ is an adjacent simplex, then $\xi_{\{\mathrm{u,v}\}}(\sigma)$ is the simplex formed by replacing v with u. For bystander simplex σ, we define $\xi_{\{\mathrm{u,v}\}}(\sigma)$ to be σ. For vanishing simplices σ with nonvanishing facet τ, we define $\xi_{\{\mathrm{u,v}\}}(\sigma) = \xi_{\{\mathrm{u,v}\}}(\tau)$. This is somewhat intuitive: consider the vanishing triangles in Figure 7. Each triangle has two facets which are mirrors. The triangle is mapped to the same simplex as the mirrors are. Similarly, $\{u, v\}$ is mapped to the same simplex as u and v.

4.3 Induced vector field

Now that a contraction operator is defined on K, it is necessary to define how a vector field is induced on K'. We define $V(K)$ to be the discrete Morse vector field on K. Hence, $V(K)$ is a set of pairs of simplices $\{\sigma, \tau\}$ where σ is a facet of τ. We use the elements of $V(K)$ together with $\xi_{\{u,v\}}$ to define the elements of $V(K')$, a discrete Morse vector field on K'. We often refer to $V(K')$ as the *induced vector field*. In particular, if $\{\sigma, \tau\} \in V(K)$, and both σ and τ are nonlocal to $\{u, v\}$, then $\{\xi_{\{u,v\}}(\sigma), \xi_{\{u,v\}}(\tau)\} = \{\sigma, \tau\} \in V(K')$. However, if either σ or τ is local to $\{u, v\}$, more care is needed.

When vectors on mirrored edges are of different types, it is necessary to choose which vector induces a member of $V(K')$. For example, if a pair of mirrored edges τ_1, τ_2 target distinct adjacent simplices, then it is necessary to decide which adjacent simplex in K' is targeted by $\xi_{\{u,v\}}(\tau_1) = \xi_{\{u,v\}}(\tau_2)$. Note that there are four distinct types of discrete Morse vectors involving mirrored edges.

- Bystander tail, Mirrored head
- Mirrored tail, Adjacent head
- Mirrored tail, Vanishing head
- Mirrored tail, Mirrored head

In addition, there is the possibility that one or both of the mirrors is critical. When confronted with such choices, we choose to assign vectors to the image of the mirrored edges with the following priority.

1. Bystander tail, Mirrored head
2. Mirrored tail, Mirrored head
3. Mirrored tail, Adjacent head
4. Critical edge

Note that because it is not possible for two mirrored simplices to target the same vanishing simplex, there is always some alternative to take. We choose this alternative. In addition, there is the possibility that both mirrors target adjacent simplices and it is necessary to choose which adjacent simplex to target. We choose not to contract in such circumstances. For mirrored vertices u, v, it may be that highest priority vector is not compatible with the vectors already assigned to the mirrored edges. Hence, we choose the highest priority compatible vector. It is easy to see that this method of assigning discrete Morse vectors defines a unique gradient vector field $V(K')$. An example of how vectors are assigned in K' can be seen in Figure 8.

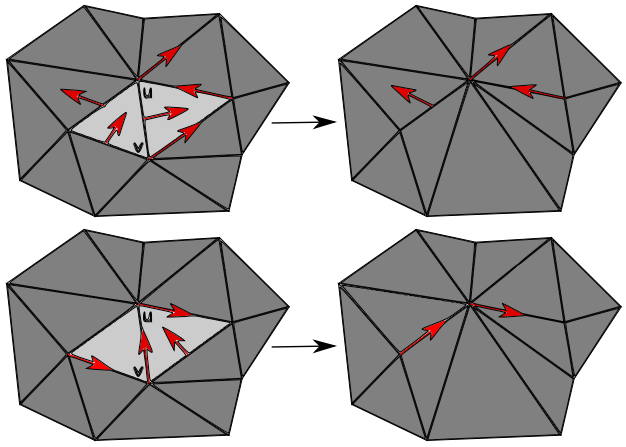

Figure 8: An example of how discrete Morse vectors are assigned on mirrored edges when contracting edge $\{u, v\}$. For the left vanishing triangle in the top left image, note that one mirror targets an adjacent triangle (priority 3) and its partner targets a vanishing triangle (last priority). Hence, the image of the mirrored edges targets the image of the adjacent simplex.

4.4 Link condition

Note that in certain cases, it is possible that contracting an edge can change the topology of K. That is, there are possible edges for which K is a 2-manifold, but K' is not. The algorithm outlined in Section 3 is only guaranteed to work on 2-manifolds, so it is critical that K' is also a 2-manifold. To ensure this, we require that $\{u, v\}$ meets the link condition [6]. Let $\text{Star}(\sigma)$ denote the set of all simplices with σ as a face. Recall that the closure $\text{Cl}(A)$ of a set of simplices A is A together with every simplex that is a face of an element of A. Define the link $\text{Lk}(\sigma)$ of a simplex σ to be $\text{Cl}(\text{Star}(\sigma)) \setminus \text{Star}(\text{Cl}(\sigma))$.

Definition 8 (Link Condition). *An edge $e = \{u, v\}$ satisfies the link condition if $\text{Lk}(e) = \text{Lk}(u) \cap \text{Lk}(v)$. We say e is contractible if it satisfies the link condition.*

For further discussion on the link condition, we refer the reader to [6].

4.5 Contraction criteria

We now have established a sufficient foundation such that we can establish criteria for contraction. In doing so, we aim for our contraction to accomplish three main objectives:

1. The induced vector field $V(K')$ is a valid discrete Morse vector field. Equivalently, $V(K')$ contains no cycles.

2. The contraction operator does not introduce any new critical simplices.

3. If $V(K)$ is the gradient vector field induced by filtration $K_0 \subseteq K_1 \subseteq \ldots \subseteq K_m = K$ for some δ, then $V(K')$ is induced by the filtration $\xi_{\{u,v\}}(K_0) \subseteq \xi_{\{u,v\}}(K_1) \subseteq \ldots \subseteq \xi_{\{u,v\}}(K_m)$ with the same δ.

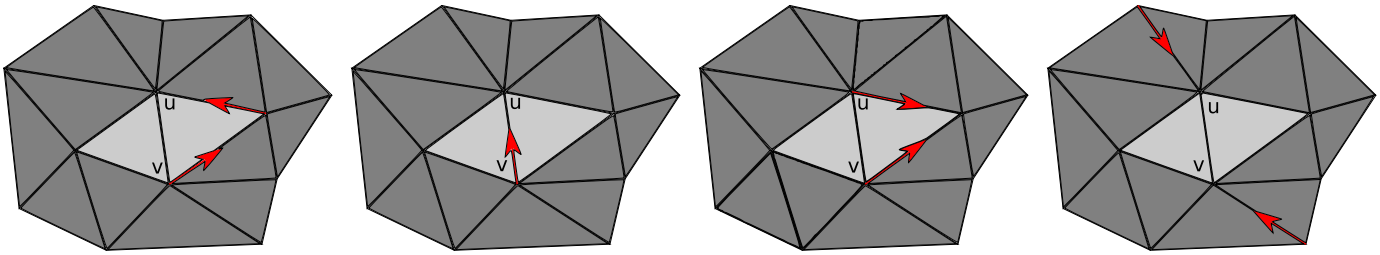

Figure 9: Vertices u, v are admissible by way of a local gradient path from v to u (first left, second left), a local gradient path from v and u to a bystander (second right), and by $\{u, v\}$ being part of the edge-vertex spanning tree and $\{u, v\}, u, v$ all being critical (far right).

In principle, we aim to establish an easily checkable set of criteria on simplices local to some edge $e = \{u, v\}$ to determine if contracting e will satisfy the given objectives. To do so, we define the following terms.

Definition 9 (Admissible Triangle). *A vanishing triangle t relative to $e = \{u, v\}$ is said to be an admissible triangle if one of the following conditions is met:*

- *Neither mirror facet of t relative to e is the tail of a vector with a head that is an adjacent simplex.*
- *One mirror facet of t targets an adjacent triangle, and the other mirror facet targets t.*

The vanishing triangles in Figure 8 are admissible. Requiring vanishing triangles to be admissible means we will not have to choose between competing mirrored/adjacent vectors.

Definition 10 (Admissible Vertices). *For edge $\{u, v\}$, the pair of vertices u, v are said to be admissible vertices if at least one of the following conditions is met.*

1. *There exists a local V-path from u to v*
2. *There exists a local V-path from v to u*
3. *There exist local V-paths from u and v to some bystander vertex r*
4. *u and v are both critical and $\{u, v\}$ is critical and paired with a vertex in the persistence sense*

By "local" V-path, we mean a gradient path where all simplices are local. Notice that for u, v to be be admissible vertices requires the existence of a path in the vertex/edge spanning tree from u to v. Examples can be seen in Figure 9

These definitions, together with the link condition, constitute our criteria.

Definition 11 (Admissible Edge). *An edge $e = \{u, v\}$ is an admissible edge if both incident triangles are admissible triangles, u, v are admissible vertices, and $\{u, v\}$ is contractible.*

Only admissible edges are candidates for contraction.

5 Theoretical guarantee

We now show that the induced vector field satisfies the stated objectives. We take K to be a triangulated 2-manifold, and define K', $V(K)$, and $V(K')$ as in Section 4.

Theorem 12. *If $e = \{u, v\}$ is an admissible edge, and $V(K)$ is a discrete Morse vector field over K, then the vector field $V(K')$ induced by $\xi_{\{u,v\}}$ is a valid discrete Morse vector field over K'.*

Proof. Aiming for a contradiction, we assume that $V(K')$ is not a valid discrete Morse vector field. Therefore, there are two cases: $V(K')$ admits either a nontrivial closed vertex/edge gradient path or a nontrivial closed triangle/edge gradient path.

First, assume that $V(K')$ admits a nontrivial closed triangle/edge gradient path. Note that all those vectors in $V(K)$ for which both the head and the tail are nonlocal to $\{u, v\}$ are also in $V(K')$. Therefore, the closed edge/triangle gradient path must contain an edge σ, where $\sigma = \xi_{\{u,v\}}(\tau_1) = \xi_{\{u,v\}}(\tau_2)$ and τ_1 and τ_2 are mirrors relative to e.

Hence, consider the closed edge/triangle gradient path $\sigma, t_1, e_1, t_2, e_2, \ldots, t_n, \sigma$. Because σ targets t_1, it follows that there exists a vector with tail τ_1 or τ_2 and head $\xi^{-1}_{\{u,v\}}(t_1)$ in $V(K)$. Without loss of generality, we assume that the vector $\{\tau_1, \xi^{-1}_{\{u,v\}}(t_1)\} \in V(K)$. But because both triangles incident to e are admissible, this implies that there is a vector in $V(K)$ with tail at τ_2 and head at the vanishing triangle between τ_1 and τ_2, which we call t. Therefore, since those triangles incident to e are admissible, $V(K)$ admits a gradient path τ_1, t, τ_2. But this implies that $V(K)$ admits a nontrivial closed gradient path $\tau_1, t, \tau_2, {\xi_{\{u,v\}}}^{-1}(t_1), \xi^{-1}_{\{u,v\}}(e_1), \ldots, \xi^{-1}_{\{u,v\}}(t_m), \tau_1$, which contradicts $V(K)$ being a valid discrete Morse vector field.

Note that there is also a case where the closed gradient path in $V(K')$ contains two simplices which are the images of mirrors, but the argument is almost exactly the same, so we omit it.

The argument concerning a vertex/edge gradient path is largely the same as the triangle/edge case. If there were a nontrivial closed vertex/edge gradient path in $V(K')$, then $\xi_{\{u,v\}}(u) = \xi_{\{u,v\}}(v)$ must be an element of the path. But because u, v are admissible vertices, there must be a path in the spanning tree from u to v containing only local simplices. Edge/vertex gradient paths are built on the spanning tree discussed in Section 3, so a closed gradient path in $V(K')$ implies that there is a cycle in the spanning tree built on K which is clearly a contradiction. □

Theorem 13. *The number of critical simplices in K' as determined by $V(K')$ is no more than the number of critical simplices in K as determined by $V(K)$.*

Proof. Note that a simplex $\sigma \in K'$ is only critical if an element of $\xi^{-1}_{\{u,v\}}(\sigma)$ is critical. Hence, the total number of critical simplices can only decrease. □

The next theorem is our main theoretical result, which essentially implies that new vector field induced by a contraction can be constructed from the old one only by local operations.

Theorem 14. *If $V(K)$ is a discrete Morse vector field induced by the filtration $K_0 \subseteq K_1 \subseteq \ldots \subseteq K_m = K$ and some δ via Algorithm 1, and $V(K')$ is the discrete Morse vector field*

induced by $V(K)$ and contracting admissible edge $\{u, v\}$, then the filtration $\xi_{\{u,v\}}(K_0) \subseteq \xi_{\{u,v\}}(K_1) \subseteq \ldots \subseteq \xi_{\{u,v\}}(K_m) = K'$ and δ induce discrete Morse vector field $V(K')$ on K'.

The proof for this theorem is significantly more involved, so we break the proof into multiple lemmas.

The first stage in showing Theorem 14 to be true is to demonstrate that there is a correspondence between the vertex/edge minimum spanning tree that is constructed in K and the vertex/edge minimum spanning tree that is constructed in K'. We refer to the former as T and the later as T'. The trees T and T' are both constructed by building a minimum spanning tree with the filtration $K_0 \subseteq K_1 \subseteq \ldots \subseteq K_m$ in the case of T and $\xi_{\{u,v\}}(K_0) \subseteq \xi_{\{u,v\}}(K_1) \subseteq \ldots \subseteq \xi_{\{u,v\}}(K_m)$ in the case of T'. In particular, we define T_i and T'_i to be the minimum spanning forest constructed by only considering those sublevel sets with indices $\leq i$. Hence, $T_0 \subseteq T_1 \subseteq T_2 \subseteq \ldots \subseteq T_m = T$ and $T'_0 \subseteq T'_1 \subseteq T'_2 \subseteq \ldots \subseteq T'_m = T'$. We let $E(T)$ denote the edge set of a tree T. These definitions give the following result.

Lemma 15. *Let T, T', T_i, T'_i be defined as above. For all i, $E(\xi_{\{u,v\}}(T_i)) = E(T'_i)$.*

Proof. We proceed by induction on i. Note that $K_0 = \emptyset$, so $\xi_{\{u,v\}}(K_0) = \emptyset$, and it immediately follows that $E(T'_0) = E(\xi_{\{u,v\}}(T_0)) = \emptyset$.

We now assume that $E(\xi_{\{u,v\}}(T_i)) = E(T'_i)$ and aim to show that $E(\xi_{\{u,v\}}(T_{i+1})) = E(T'_{i+1})$. If $T_i = T_{i+1}$, then we are done. Hence, assume that $e_{i+1} \in T_{i+1}$ but $e_{i+1} \notin T_i$. In the case where e_{i+1} is vanishing, the result is immediate, as $\xi_{\{u,v\}}(e_{i+1})$ is a vertex. If e_{i+1} is a mirrored simplex which occurs after its partner in the filtration, then the image of the lesser mirror must already be part of the forest, and hence $\xi_{\{u,v\}}(e_{i+1}) \in E(T_i)$, and the proof follows by the inductive hypothesis. If e_{i+1} is a mirror that precedes its mirror, or a nonlocal edge, and e_{i+1} joins two trees in the forest built over K, then it follows that $\xi_{\{u,v\}}(e_{i+1})$ must also. Else, $\xi_{\{u,v\}}(e_{i+1})$ causes a cycle in the vertex/edge spanning tree on K', which is not possible because this implies a cycle in the spanning tree on K because vertex admissibility requires a path in the spanning tree from u to v. But this implies that e_{i+1} does not join two trees in the spanning forest, which contradicts our assumption. □

This result immediately implies the following.

Corollary 16. *Let $e = \{r, s\}$ be an edge in K which is either a nonlocal simplex or a mirror which occurs earlier in the filtration than its partner. If after introducing e to T there exists a path from vertex r to some vertex x, then after introducing $\xi_{\{u,v\}}(e)$ there exists a path in T' from $\xi_{\{u,v\}}(r)$ to $\xi_{\{u,v\}}(x)$.*

We reference this corollary frequently in the remaining theorems.

For the next result, we define $\tau, \tau', \tau_i, \tau'_i$ analogously to T, T', T_i, T'_i but for the triangle/edge spanning forest. The result follows from essentially the same argument as Lemma 15, while controlling for the fact that when one mirrored simplex is in the triangle spanning tree and the other is in the vertex spanning tree, their image is in the vertex spanning tree.

Lemma 17. *Let $\tau, \tau', \tau_i, \tau'_i, T'$ be defined as above. For all i, $E(\xi_{\{u,v\}}(\tau_i)) \setminus E(T') = E(\tau'_i)$.*

While the previous two results show that the induced trees are the same, that is not to say that the induced forests are the same. What remains to be shown is that for edge $e \neq \{u, v\}$, and e not a mirrored simplex which succeeds its partner in the total order, $\text{Pers}(e) \leq \delta$ if and only if $\text{Pers}(\xi_{\{u,v\}}(e)) \leq \delta$. In the following proofs, we say that a simplex σ is *introduced* at stage i if the simplex $\sigma \in K_i, \sigma \notin K_{i-1}$. Simplex σ is *introduced after* simplex τ if σ is introduced at stage i and τ is introduced at stage $j < i$. In addition, when we introduce an edge e, we use $\text{MaxV}, \text{MinV}, \text{MaxT}, \text{MinT}$ to refer to the roots of the trees that the edge has joined: MaxV refers to the vertex root with the greater height value, MaxT refers to the triangle root with the greater height value, and MinT and MinV are defined as expected. In addition, we use the notation $h : K \to \mathbb{R}$ and $h' : K' \to \mathbb{R}$ to reflect the height value of a simplex in K, K' respectively.

Lemma 18. *For edge $e \neq \{u, v\}$ which is not a mirrored simplex introduced after its partner, $h'(\text{MaxV}(\xi_{\{u,v\}}(e))) \leq h(\text{MaxV}(e))$ and $h'(\text{MinV}(\xi_{\{u,v\}}(e))) \leq h(\text{MinV}(e))$.*

Proof. When $e = \{r, s\}$ is introduced to the spanning tree, there exists a path in the tree from r to $\text{MaxV}(e)$ and s to $\text{MinV}(e)$ or vice-versa. Therefore, by Corollary 16, when $\xi_{\{u,v\}}(e)$ is introduced, there exists a path from $\xi_{\{u,v\}}(r)$ and $\xi_{\{u,v\}}(s)$ to $\xi_{\{u,v\}}(\text{MaxV}(e))$ and $\xi_{\{u,v\}}(\text{MinV}(e))$. $\text{MinV}(e)$ and $\text{MaxV}(e)$ refer to the minimum value in their respective trees, and vertices can only reduce in value under $\xi_{\{u,v\}}$, so the proof follows. □

We prove a similar lemma for the edge/triangle tree.

Lemma 19. *For edge $e \neq \{u, v\}$ which is not a mirrored simplex introduced after its partner, $h'(\text{MaxT}(\xi_{\{u,v\}}(e))) \leq h(\text{MaxT}(e))$ and $h'(\text{MinT}(\xi_{\{u,v\}}(e))) \leq h(\text{MinT}(e))$.*

Proof. When an edge e is introduced, it forms a bridge between two triangle/edge trees. But contracting an edge cannot merge two of these trees, because the image of a pair of mirrors takes the place in the total order of whichever came first. But contracting can destroy triangles that were $\text{MinT}(e)$ or $\text{MaxT}(e)$ for some edge e. Hence, the value of the maximum triangle in each tree in the forest can only be reduced, and the lemma follows. □

Recall that the persistence algorithm pairs simplices σ, τ where τ destroys a homological class created by σ. An edge can pair with a vertex or a triangle depending on if it destroys or creates a homological class. This is equivalent to saying that e is in the vertex/edge or triangle/edge spanning tree, respectively.

The next two lemmas follow immediately from the previous two, and the fact that $\text{Pers}(e) = h(e) - h(\text{MaxV}(e))$ for edges paired with vertices and $\text{Pers}(e) = h(\text{MinT}(e)) - h(e)$ for edges paired with triangles.

Lemma 20. *Let $e \neq \{u, v\}$ be an edge paired with a triangle and not a mirrored simplex introduced after its partner. If $\text{Pers}(e) < \delta$, then $\text{Pers}(\xi_{\{u,v\}}(e)) < \delta$.*

Lemma 21. *Let $e \neq \{u, v\}$ be an edge paired with a vertex and not a mirrored simplex introduced after its partner. If $\text{Pers}(e) \geq \delta$, then $\text{Pers}(\xi_{\{u,v\}}(e)) \geq \delta$.*

The following two lemmas complete the proof of Theorem 14.

Lemma 22. *Let $e \neq \{u, v\}$ be an edge paired with a triangle and not a mirrored simplex introduced after its partner. If* $\text{Pers}(e) \geq \delta$*, then* $\text{Pers}(\xi_{\{u,v\}}(e)) \geq \delta$.

Proof. Note that $\text{Pers}(e) = h(\text{MinT}(e)) - h(e)$. Because e is nonlocal or mirrored with lower height value than its partner, $h'(\xi_{\{u,v\}}(e)) = h(e)$. Therefore, the only way that $\text{Pers}(e) \geq \delta$ but $\text{Pers}(\xi_{\{u,v\}}(e)) < \delta$ is if $h'(\text{MinT}(\xi_{\{u,v\}}(e))) < h(\text{MinT}(e))$. Note that because e is critical, $\text{MinT}(e)$ must also be critical. Because the mirror which survives the contraction is introduced first, and Kruskal's is building a maximum spanning tree, it follows that $\text{MinT}(e)$ must be a vanishing simplex relative to $\{u, v\}$. But the only critical triangles which are destroyed by contraction are isolated. That is, they can only reach other local simplices via V-Paths. Therefore, there must be some local edge ω where $h(\omega) \geq h(e)$ such that ω is critical. In addition, $h(\text{MinT}(\omega)) \leq h(\text{MinT}(e))$, as ω was not paired with $\text{MinT}(e)$, but connected to its tree. Therefore, because $h(\text{MinT}(\omega)) - h(\omega) \geq \delta$, where $h(\text{MinT}(\omega)) \leq h(\text{MinT}(e))$ and $h(\omega) \geq h(e)$, it follows that $h'(\text{MinT}(\xi_{\{u,v\}}(e)) - h'(\xi_{\{u,v\}}(e)) \geq \delta$. □

Lemma 23. *Let $e \neq \{u, v\}$ be an edge paired with a vertex and not a mirrored simplex introduced after its partner. If* $\text{Pers}(e) < \delta$*, then* $\text{Pers}(\xi_{\{u,v\}}(e)) < \delta$.

Proof. First we consider the cases where u, v are admissible vertices because there exists a local V-path from u to v or vice-versa. Label the edge in the path which occurs latest in the total order on K as ω. If $\omega \prec e$, then the lemma follows trivially, as upon the introduction of ω, there is already a path in the spanning tree between u to v, so contraction does not make new areas accessible. Hence, $\xi_{\{u,v\}}(\text{MaxV}(e)) = \text{MaxV}(\xi_{\{u,v\}}(e))$, and lemma follows. Thus, we assume that $e \prec \omega$. In such a case, then contracting $\{u, v\}$ may complete a path so that vertex $\xi_{\{u,v\}}(r)$ is reachable from $\xi_{\{u,v\}}(e)$ upon its introduction, but r is not reachable from e. Note, however, that if it were the case that $\text{Pers}(\xi_{\{u,v\}}(e)) \leq \delta$, then it necessarily follows that $h(\text{MaxV}(\omega)) \leq h'(\text{MaxV}(\xi_{\{u,v\}}(e))$. Because by assumption, ω has associated persistence less than δ, it follows that $h(\omega) - h(\text{MaxV}(\omega)) < \delta$. But $h'(\xi_{\{u,v\}}(e)) \leq h(\omega)$, so it follows that $h'(\xi_{\{u,v\}}(e)) - h(\text{MaxV}(\omega)) < \delta$. Similarly, $h'(\text{MaxV}(\xi_{\{u,v\}}(e)) \geq h(\text{MaxV}(\omega))$, so it follows that $h'(\xi_{\{u,v\}}(e)) - h'(\text{MaxV}(\xi_{\{u,v\}}(e))) < \delta$. The case where there is a path from u, v to a bystander vertex follows analogously.

Now, we consider the case where u, v are admissible vertices because u is critical, v is critical, and $\{u, v\}$ is critical and paired with a vertex in the persistence sense. In addition, we note that a vertex-edge is critical if and only if it is paired with a critical vertex in the persistence sense. Hence, because $\text{Pers}(e) < \delta$, e is paired with neither u nor v. But contracting u into v only lowers the value of their image, and thus $\xi_{\{u,v\}}(\text{MaxV}(e)) = \text{MaxV}(\xi_{\{u,v\}}(e))$. Hence, $h'(\text{MaxV}(\xi_{\{u,v\}}(e)) = h(\text{MaxV}(e))$, so $\text{Pers}(e) < \delta$. □

So because forests maintain their structure and the operator assigns vectors that point along V-paths to minimum vertices and maximum triangles, Theorem 14 follows immediately.

6 Experimental results

In this section, the new contraction criteria is compared to those presented in [16], and the theoretical guarantee's utility is demonstrated for applications that rely on extracting 1-unstable manifolds.

Dataset	Initial Simplices	New Remaining Simplices	[16] Remaining Simplices	% Reduction
Columbus	2,728,353	83,970.8	124,984.6	32.82
Los Alamos	2,728,353	49,106.6	74,756.6	34.31
Minneapolis	10,940,401	123,200.4	190,027.4	35.17
Aspen	10,940,401	48,418.8	62,778.8	22.87
Filigree	3,086,440	394,095.8	577,172.4	31.72
Isidore	6,626,810	822,053.2	1,159,809.8	29.12
Eros	2,859,566	361,723.8	516,992.2	30.03

Table 1: Coarseness data for $\delta = \epsilon$, where every edge with positive associated persistence is critical.

Dataset	Initial Simplices	New Remaining Simplices	[16] Remaining Simplices	% Reduction
Columbus	2,728,353	15,609	16,065	2.84
Los Alamos	2,728,353	14,853	15,039	1.24
Minneapolis	10,940,401	33,703	34,669	2.79
Aspen	10,940,401	33,313	33,409	.29
Filigree	3,086,440	2,426.2	2,919.2	16.89
Isidore	6,626,810	8	8	0
Eros	2,859,566	20	20	0

Table 2: Coarseness data for $\delta = \infty$.

6.1 Unstable manifolds

Extracting the *unstable* 1-*manifolds* of a discrete Morse vector field has been used by various authors for applications in cosmology, image skeletonization, and road network reconstruction [24, 25, 5]. An unstable 1-manifold is the set of all edges that can be reached from a gradient path originating at a given critical edge. In [25], the authors showed that the unstable 1-manifolds of a complex built from GPS trajectories correspond to a city's roads. We show a result about the structure of these unstable 1-manifolds under our contraction operator.

Theorem 24. *Let K, K', $V(K)$, and $V(K')$ be defined as in Section 4. For triangulated manifold K equipped with vector field $V(K)$, define $U_1(K, V(K))$ to be the set of simplices*

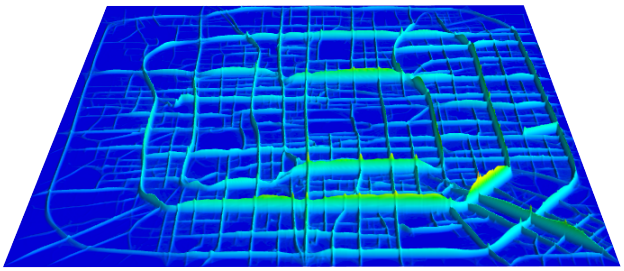

Figure 10: Frequency data corresponding to Beijing. Elevation corresponds to the number of times that a GPS trajectory was recorded as colliding with the given point.

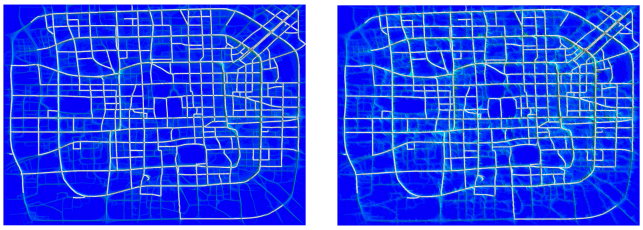

Figure 11: A map of Beijing before (left, 22.5 million simplices) and after contraction (right, 1.5 million simplices) together with the unstable manifolds of all critical edges marked in white. Note that the unstable manifolds maintain their structure after contraction.

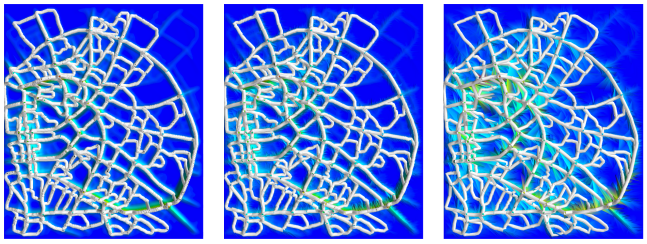

Figure 12: The unstable manifolds corresponding to a map of Berlin, marked in white, with 1.97 million simplices (left), 456,000 simplices (middle), and 156,000 simplices(right).

in unstable 1*-manifolds on* K*. Then* $U_1(K', V(K')) \subseteq \xi_{\{u,v\}}(U_1(K, V(K)))$.

Proof. Consider $\sigma \in U_1(K', V(K'))$. We aim to show that $\sigma \in \xi_{\{u,v\}}(U_1(K, V(K)))$. Since σ is in an unstable manifold, there exists some critical edge $e \in K'$ connected to σ by a gradient path. Denote this gradient path $e = e_1, v_1, \ldots, \sigma$. Since e is critical, by the proof of Theorem 13, an edge in $\xi^{-1}_{\{u,v\}}(e)$ must be critical. We claim that there exists a gradient path from some critical edge in $\xi^{-1}_{\{u,v\}}(e)$ to some element of $\xi^{-1}_{\{u,v\}}(\sigma)$. This follows from considering the preimages of the gradient path. If every simplex in the path is the image of nonlocal simplices to $\{u, v\}$, then the preimage of the gradient path is a gradient path connecting $\xi^{-1}_{\{u,v\}}(e)$ to $\xi^{-1}_{\{u,v\}}(\sigma)$, so $\xi^{-1}_{\{u,v\}}(\sigma) \in U_1(K, V(K))$ implying $\sigma \in \xi_{\{u,v\}}(U_1(K, V(K)))$.

Hence, we assume that some element of the path is the image of simplices local to $\{u, v\}$. Note that no simplex in the path other than σ or e can be the image of mirrored critical simplices. If some simplex $\tau \neq e, \sigma$ were the image of mirrored critical simplices, τ would necessarily be critical and the gradient path could not proceed beyond τ. Hence, u and v are not both critical unless u, v map to σ, in which case the preimage of the gradient path connects a critical edge in $\xi^{-1}_{\{u,v\}}(e)$ to u or v, and we are done. Thus, assume there is a gradient path from u to v or vice-versa, or there is a path from each of u and v to some bystander vertex. The preimage of the gradient path $\xi^{-1}_{\{u,v\}}(e_1), \xi^{-1}_{\{u,v\}}(v_1), \ldots, \xi^{-1}_{\{u,v\}}(\sigma)$ is not a gradient path, as for some vertex v_i, $\xi^{-1}_{\{u,v\}}(v_i)$ contains two vertices. We use the path guaranteed by vertex admissibility to fill the gap as needed, which then completes a path from $\xi^{-1}_{\{u,v\}}(e_1)$ to $\xi^{-1}_{\{u,v\}}(\sigma)$ in K. Hence, $\xi^{-1}_{\{u,v\}}(\sigma) \in U_1(K, V(K))$ implying $\sigma \in \xi_{\{u,v\}}(U_1(K, V(K)))$. □

The image of critical mirrors under $\xi_{\{u,v\}}$ may not be critical, so equality is not guaranteed in Theorem 24. Experimentally, we show that it makes little difference in practice.

Comparisons of computing the unstable manifolds on the complex before and after contraction can be seen in Figures 2,11,12, and 13. Notice that the unstable 1-manifolds in Figure 2 do not follow the "mountain ridges," whilst those in Figure 11 do. To achieve this effect, vertices are treated as if they had the negative of their function value. For a more thorough treatment, we refer the reader to [25] or [7].

As the number of edges contracted increases, the accuracy of the unstable 1-manifolds decreases. This is illustrated in Figures 11, 12, and 13. While the structure of the unstable manifolds largely stays the same, a coarser representation contains fewer vertices, and hence it results in a worse representation of the manifolds. Nevertheless, even at very coarse representations, the unstable manifolds remain a good approximation. Notice that if the only goal was to simplify the unstable 1-manifolds while maintaining their structure, then an alternative approach would be to extract the unstable manifolds and simplify the induced graph directly rather than dealing with the entire complex. But such an approach does not provide a guarantee on the structure of the unstable manifolds in the contracted complex.

6.2 Granularity

As the new criteria subsume those which are given in [16], the new criteria permit for a coarser representation of the triangulated manifold while still maintaining the structure of the discrete Morse vector field. To test this, a discrete Morse vector field is assigned to a triangulated dataset by the procedure described in Section 3 with some δ, and admissible edges are contracted in a random order until none of the remaining edges are admissible. We also experimented with contracting edges in order of their associated persistence, but found that contracting in a random order did a much better job of preserving the quality of the triangulation. A more thorough investigation of the impact of the edge contraction order is left to future work. The resulting granularity is compared for $\delta = \infty$ and $\delta = \epsilon$, where ϵ is chosen such that only those edges with persistence equal to 0 are not critical. Datasets are either terrains (Aspen, Los Alamos, Columbus, Minneapolis) and courtesy of the National Elevation Dataset, or 2-manifolds without boundary, courtesy of the Aim@Shape repository. The algorithm from Section 3 requires a height function defined on the vertices of the triangulation, so the vertices of those datasets which are 2-manifolds without boundary are equipped with a curvature approximation. Note that in the case of the terrains, we do not contract edges on the boundary, as the link condition only applies when the edge is not on the boundary [6].

Resulting data can be found in Table 1 for $\delta = \epsilon$ and Table 2 for $\delta = \infty$. Note that for $\delta = \epsilon$, the new contraction criteria presents around a 30% reduction in simplices when compared to the criteria presented in [16]. For $\delta = \infty$, the reduction is much more modest. Applying Algorithm 1 with $\delta = \epsilon$ results in many critical simplices, while $\delta = \infty$ produces the minimum possible. Hence, these experiments demonstrate that much of the improvement over the criteria in [16] comes from our contraction operator's ability to destroy critical simplices. Contraction images can be viewed in Figure 14 and Figure 15.

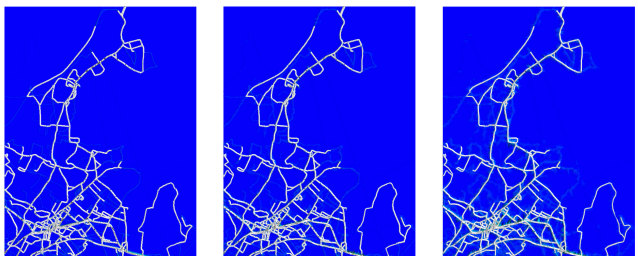

Figure 13: The unstable manifolds corresponding to a map of Athens with 2.7 million simplices (left), 860,000 simplices (middle), and 262,000 simplices(right).

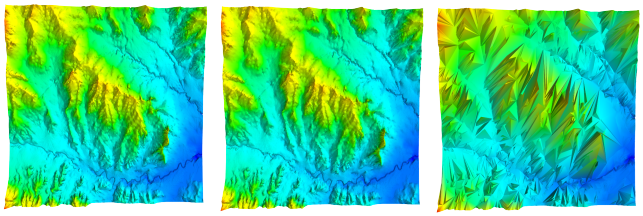

Figure 14: A terrain near Los Alamos, New Mexico with 2.7 million simplices (left), 1.5 million simplices (middle), and 15,000 simplices(right).

Figure 15: The original Filigree dataset (top left 3.1 million simplices), the contracted Filigree dataset (bottom left - 400,000 simplices), the original Eros dataset (top center - 2.8 million simplices), the contracted Eros dataset (bottom center - 100,000 simplices), the original Isidore dataset (top right - 6.6 million simplices), and the contracted Isidore dataset (bottom right - 1.1 million simplices).

7 Conclusion

7.1 Future work

Many open questions ensue from this work. This paper has developed a contraction operator such that the resulting discrete Morse vector field is the same as the vector field induced by the image of the filtration under the contraction map. A more general version of this problem is to develop a contraction operator which controls the perturbation of the underlying discrete Morse function.

Another natural extension to this work is to prove analogous results for algorithms that generate discrete Morse vector fields on 2-complexes or higher dimensional manifolds. It has been shown in [20] and [17] that computing an optimal discrete Morse vector field on an arbitrary 2-complex is NP-hard, so it is natural to begin by proving such results for non-optimal Morse vector fields. We plan to explore this direction in the future. In addition, discrete Morse vector fields on higher dimensional manifolds have been explored in [20] and [23]. The former presents a heuristic for 3-manifolds, while the later guarantees optimality for specific cubical complexes. We are currently investigating if it is possible to prove results analogous to the ones presented in this paper for those algorithms.

It may be possible to expand the contractibility criteria substantially if the definition of "local" is relaxed. This is of particular interest when $\{u, v\}$ is critical. It may not be necessary to require u and v each to be critical, but then additional information is needed to guarantee that contraction does not cause a closed gradient path.

The authors of [16] established a data structure for storing a hierarchy of discrete Morse vector fields across edge contractions. Permitting additional cases requires more memory in the data structure, as every contraction must be reversible. At the very least, the experiments in Section 6 suggest that it may be worth incorporating contractions which destroy critical edges.

7.2 Acknowledgments

The authors would like to thank INRIA for their models found at the Aim@Shape repository, the National Elevation Dataset for their terrain data, and Suyi, Jiayuan, and Yusu Wang for their GPS datasets. In addition, the authors want to acknowledge several anonymous reviewers for their helpful comments. This work was partially supported by NSF grants CCF-1740761, CCF-1526513, and DMS-1547357.

References

[1] D. Attali, M. Glisse, D. Morozov, S. Hornus, and F. Lazarus. Persistence-sensitive simplification of functions on surfaces in linear time. Appeared in workshop TopoInVis, 2009.

[2] U. Bauer, C. Lange, and M. Wardetzky. Optimal topological simplification of discrete functions on surfaces. *Discrete & Computational Geometry*, 47(2):347–377, Mar 2012.

[3] P.-T. Bremer, V. Pascucci, and B. Hamann. *Maximizing Adaptivity in Hierarchical Topological Models Using Cancellation Trees*, pages 1–18. Springer Berlin Heidelberg, Berlin, Heidelberg, 2009.

[4] L. Ćomić, L. De Floriani, F. Iuricich, and P. Magillo. Computing a discrete morse gradient from a watershed decomposition. *Comput. Graph.*, 58(C):43–52, Aug. 2016.

[5] O. Delgado-Friedrichs, V. Robins, and A. Sheppard. Skeletonization and partitioning of digital images using discrete morse theory. *IEEE Transactions on Pattern Analysis and Machine Intelligence*, 37:654–666, 03 2015.

[6] T. K. Dey, H. Edelsbrunner, S. Guha, and D. V. Nekhayev. Topology preserving edge contraction. *Publ. Inst. Math.(Beograd)(NS)*, 66(80):23–45, 1999.

[7] T. K. Dey, J. Wang, and Y. Wang. Improved road network reconstruction using discrete morse theory. In *Proceedings of the 25th ACM SIGSPATIAL International Conference on Advances in Geographic Information Systems, GIS 2017, Redondo Beach, CA, USA, November 7-10, 2017*, pages 58:1–58:4, 2017.

[8] T. K. Dey, J. Wang, and Y. Wang. Graph reconstruction by discrete morse theory. To appear in Proceedings of the 34th International Symposium on Computational Geometry (SoCG'18), 2018.

[9] H. Edelsbrunner and J. Harer. *Computational Topology: An Introduction*. 01 2010.

[10] H. Edelsbrunner, J. Harer, and A. Zomorodian. Hierarchical morse-smale complexes for piecewise linear 2-manifolds. *Discrete and Computational Geometry*, 30:87–107, 07 2003.

[11] H. Edelsbrunner, D. Letscher, and A. Zomorodian. Topological persistence and simplification. *Discrete & Computational Geometry*, 28(4):511–533, Nov 2002.

[12] R. Fellegara, F. luricich, L. De Floriani, and K. Weiss. Efficient computation and simplification of discrete morse decompositions on triangulated terrains. In *Proceedings of the 22Nd ACM SIGSPATIAL International Conference on Advances in Geographic Information Systems*, SIGSPATIAL '14, pages 223–232, New York, NY, USA, 2014. ACM.

[13] R. Forman. Morse theory for cell complexes. *Advances in Mathematics*, 134(1):90 – 145, 1998.

[14] R. Forman. A user's guide to discrete morse theory. In *Proc. of the 2001 Internat. Conf. on Formal Power Series and Algebraic Combinatorics, A special volume of Advances in Applied Mathematics*, page 48, 2001.

[15] A. Gyulassy, M. Duchaineau, V. Natarajan, V. Pascucci, E. Bringa, A. Higginbotham, and B. Hamann. Topologically clean distance fields. *IEEE Trans. Visualization Computer Graphics*, 13(6):1432–1439, Nov 2007.

[16] F. Iuricich and L. De Floriani. Hierarchical forman triangulation: a multiscale model for scalar field analysis. *Computers & Graphics*, 66:113–123, 06 2017.

[17] M. Joswig and M. E. Pfetsch. Computing optimal morse matchings. *SIAM Journal on Discrete Mathematics*, 20(1):11–25, 2006.

[18] H. King, K. Knudson, and N. Mramor. Generating discrete morse functions from point data. *Experimental Mathematics*, 14(4):435–444, 2005.

[19] T. Lewiner, H. Lopes, and G. Tavares. Optimal discrete morse functions for 2-manifolds. *Computational Geometry*, 26(3):221 – 233, 2003.

[20] T. Lewiner, H. Lopes, and G. Tavares. Towards optimality in discrete morse theory. *Experimental Mathematics*, 12(3):271–285, december 2003.

[21] J. Marsden, D. Ebin, and A. Fischer. *Diffeomorphism Groups, Hydrodynamics and Relativity*. 1972.

[22] J. Milnor. *Morse Theory*. Princeton University Press, 1963.

[23] V. Robins, P. J. Wood, and A. P. Sheppard. Theory and algorithms for constructing discrete morse complexes from grayscale digital images. *IEEE Transactions on Pattern Analysis and Machine Intelligence*, 33(8):1646–1658, Aug 2011.

[24] T. Sousbie. The persistent cosmic web and its filamentary structure i. theory and implementation. *Monthly Notices of the Royal Astronomical Society*, 414:350 – 383, 06 2011.

[25] S. Wang, Y. Wang, and Y. Li. Efficient map reconstruction and augmentation via topological methods. In *Proceedings of the 23rd SIGSPATIAL International Conference on Advances in Geographic Information Systems*, SIGSPATIAL '15, pages 25:1–25:10, New York, NY, USA, 2015. ACM.

[26] K. Weiss, F. Iuricich, R. Fellegara, and L. De Floriani. A primal/dual representation for discrete morse complexes on tetrahedral meshes. *Computer Graphics Forum*, 32(3pt3):361–370, 2013.